J Low Temp Phys (2016) 185:129–137
DOI 10.1007/s10909-016-1544-6

Commensurate Phases of Kr Adsorbed on Single-Walled Carbon Nanotubes

Mamadou T. Mbaye[1] · **Sidi M. Maiga**[1] · **Silvina M. Gatica**[1]

Received: 6 November 2015 / Accepted: 3 February 2016 / Published online: 22 February 2016

Abstract In this paper, we show that Krypton atoms form a commensurate solid (CS) phase with a fractional coverage of one krypton atom per every four carbons on zigzag carbon nanotubes. This is a unique phase, different from the $\sqrt{3} \times \sqrt{3}$R30° CS monolayer formed on graphite, which has a lower coverage of one krypton atom per every *six* carbons. Our prediction disagrees with experiments that observe in nanotubes the same solid structure found on graphite. In order to address this discrepancy, we simulated adsorption of Kr on zigzag and armchair single-walled carbon nanotubes with radii ranging from 4.7 to 28.83 Å. Our simulations confirm that the CS of coverage 1/4 forms on medium-sized zigzag nanotubes. We also found the 1/6-coverage solid on graphene, which represents the infinite-radius limit of a nanotube. Our findings are key to experiments of adsorption on nanotubes where the interpretation and justification of the results are based on the monolayer coverage, such as mass or conductance isotherms measurements.

Keywords Adsorption · Nanotubes · Krypton · Commensuration

1 Introduction

The investigation of adsorption phenomena has been a very exciting and successful scientific activity in the last half-century [1–9]. In recent years, a considerable amount of work has been devoted to investigate theoretically and experimentally the physical adsorption in bundles of carbon nanotubes [10–16]. While bundles of nanotubes have

✉ Silvina M. Gatica
sgatica@howard.edu

[1] Department of Physics and Astronomy, Howard University, 2355 Sixth St NW, Washington, DC 20059, USA

considerable interest, their geometry is usually unknown, making the interpretation of results burdensome. This hitch can be avoided in experiments involving gas adsorption on a single suspended nanotube [17–19].

The structure of a SWNT can be defined specifically by its chiral numbers (n, m), [20] and classified as zigzag, armchair, and chiral. $(n, 0)$ type are called zigzag nanotubes while (n, n) are called armchair nanotubes. The chiral angle θ also defines the geometry of a SWNT. Armchair and zigzag SWNTs correspond to chiral angles $\theta = 30°$ and $0°$, respectively. SWNTs with $0 < \theta < 30°$ are called chiral.

Recent experiments aimed to explore the use of carbon nanotubes as molecular sensors, report mass, and conductance isotherms of noble gases on suspended SWNTs [17–19]. The interpretation of experimental results is partially based on the expectation that the structure of the adsorbed monolayer is similar to the one formed on graphite (apart from the curvature), which has a fractional coverage $\phi = 1/6$ (ϕ is defined as the number of adsorbed atoms per carbons). We have previously reported that Kr atoms form indeed a stable commensurate solid (CS) phase on SWNTs, but with a fractional coverage $\phi = 1/4$ [21]. This phase is energetically precluded to form on a planar structure and it can only exist on a SWNT due to the finite curvature of the cylindrical surface. We also observed that this 1/4-CS phase forms on (18,0) and (21,0) zigzag SWNTs but not on a (12,12) armchair SWNT. This observation is consistent with our further studies, [22] which show that the commensuration of the substrate systematically decreases with the chiral angle. For example, an armchair $(12, 12)$ SWNT exposes the smoothest surface, compared to SWNTs with the same size ($R = 0.82$ nm) but other chiral angles including chiral $(11, 2)$ and zigzag $(21, 0)$ tubes. In this article, we report an extended study of Kr on zigzag and armchair SWNTs with radii ranging from 4.7 to 28.83 Å, with emphasis on the comparison between adsorption on tubes with same radius but different chirality. We also show results for Kr on graphene, which represents the infinite-radius limit of a SWNT.

This article is organized as follows: In Sect. 2, we present the model and method; in Sect. 3, we discuss the results, and we present our summary and conclusions in Sect. 4.

2 Method

Using the simulation technique Grand Canonical Monte Carlo (GCMC) we studied the structure of Kr atoms adsorbed on suspended zigzag and armchair SWNTs. In a GCMC simulation, the chemical potential, the temperature, and volume of the system are held constant while the number of particles varies. In the simulations, we positioned the SWNT at the center of the simulation cell, with the axis parallel to the z direction. We assume the SWNT to be a rigid infinitely long tube, which we realized by setting periodic boundary conditions on top and bottom sides of the simulation cell. The length of the simulation cell in the z direction is 80 Å and in the x, y directions is set to the diameter of the SWNT plus 40 Å. The boundary conditions are set periodic in the z direction and reflective in x, y. The input data of the simulation are the pressure of the vapor, the temperature, and the chiral numbers. The output data of the simulation are the average number of adsorbed atoms (N), the averages of the total energy, the

energy gas–surface (E_{gs}), and the energy gas–gas (E_{gg}). We also collect samples of the coordinates for each of the adsorbed atoms. For each single data point in the isotherms $N(P, T)$, we typically run 3×10^6 MC moves to reach equilibrium and 10^6 moves are performed for data collection. The ratio of creation/deletion/translation moves is 0.40/0.40/0.20.

We compute the adsorption potential as the pairwise sum of two-body interactions between individual carbon atoms and the adatom,

$$V(\vec{r}) = \sum_i U\left(|\vec{r} - \vec{R}_i|\right), \tag{1}$$

We use the Lennard-Jones (LJ) potential to model the adsorbate–adsorbate interactions, [23] with parameters $\sigma_{\mathrm{KrKr}} = 3.6$ Å and $\epsilon_{\mathrm{KrKr}} = 171$ K [24,25].

For the adatom-carbon interactions, we adopted the anisotropic pair interaction from Ref. [26]. This potential, which was developed to describe the interaction of He with graphite, is more corrugated than the isotropic LJ potential. The anisotropic potential is given by the following equation: [26]

$$U^a(r,\theta) = 4\epsilon_{\mathrm{aC}}\left(\left(\frac{\sigma_{\mathrm{aC}}}{r}\right)^{12}\left\{1+\gamma_{\mathrm{R}}\left[1-\frac{6}{5}\cos^2\theta\right]\right\} - \left(\frac{\sigma_{\mathrm{aC}}}{r}\right)^{6}\left\{1+\gamma_{\mathrm{A}}\left[1-\frac{3}{2}\cos^2\theta\right]\right\}\right), \tag{2}$$

where the parameters γ_A and γ_R determine the anisotropy of the dispersion potential that originates in the anisotropy of the π-bonds of the C atoms comprising the tube [26]. In Eq. 2, θ is the angle between the interatomic separation vector $\vec{r}$ and the radial vector, normal to the surface at the position of the ith carbon atom. The LJ parameters for the adatom-C potential are obtained by fitting physical properties of the gases and using semi-empirical combining rules: $\sigma_{\mathrm{aC}} = (\sigma_{\mathrm{aa}} + \sigma_{\mathrm{CC}})/2$ and $\epsilon_{\mathrm{aC}} = (\epsilon_{\mathrm{aa}}\epsilon_{\mathrm{CC}})^{1/2}$, [27] with $\sigma_{\mathrm{CC}} = 3.4$ Å and $\epsilon_{\mathrm{CC}} = 28$ K [24,25]. We have adopted $\gamma_A = -0.54$ and $\gamma_R = 0.38$ based on a previous study of He on graphite [26].

In a CS phase, the adsorbate atoms form an ordered array of distinct lattice sites that are correlated with the substrate. An incommensurate solid (IS) phase, on the other hand, refers to a solid structure that is uncorrelated with the substrate; the atoms are pushed away from their preferred bonding sites due to the high density of the solid.

In order to analyze the different phases of the adsorbed atoms, we first detect discontinuities or steps in the isotherms $E_{gs}(P)$ and $\phi(P)$. Once a step is detected, we quantitatively analyze the data points around the step. For step-related data points, we unroll the monolayer in a plane and calculate the 2-dimensional radial distribution function (2D-RDF) in order to determine the phase (solid or liquid), and the structure factor to evaluate the commensuration i.e., CS or IS. The 2D-RDF, $g(r)$, measures the correlation between particles within a system, and the structure factor $S(\vec{k})$ is the squared modulus of the Fourier transform of the pair correlation function (see Ref. [22] for the definition and details).

Table 1 Summary of the phases of Kr on zigzag SWNTs at $T = 77.4$ K

Structure	Radius (Å)	Transition	Coverage (ϕ range)
Zigzag (12,0)	4.74	V → L	∼1/3(0.28−0.30)
Zigzag (18,0)	6.70	V → L , L→CS	∼1/4(0.22−0.25)
Zigzag (20,0)	7.80	V → L , L→CS	∼1/4(0.22−0.25)
Zigzag (21,0)	8.20	V → L , L→CS	∼1/4(0.22−0.24)
Zigzag (33,0)	12.90	V → L , L→CS	∼1/5(0.20−0.22)
Zigzag (45,0)	17.60	V → L , L→CS	∼1/5(0.18−0.21)
Zigzag (66,0)	25.83	V → L	∼1/5(0.18−0.21)
Zigzag (69,0)	27.00	V → L	∼1/6(0.17−0.20)
Zigzag (72,0)	28.18	V → L	∼1/6(0.16−0.20)

3 Results

We first present the results of Kr on zigzag SWNTs of radii ranging from 4.74 to 28.18 Å. We summarize our findings in Table 1. In the following, the temperature in these simulations is $T = 77.4$ K, unless otherwise indicated.

For the smallest SWNT ($R = 4.74$ Å) and largest SWNTs studied ($R = 25.83$, 27.00 and 28.18 Å), we observe a V → L transition for the adsorbed Kr atoms. For the nanotubes in the intermediate size range of 6.7 to 17.6 Å there is also a L → CS transition with fractional coverage ϕ in the range 0.20 to 0.25, consistent with our previous findings on the (18,0) SWNT.

The coverage of this stable CS monolayer is approximately 1/4 Kr per carbon atoms, higher than the 1/6-CS found on graphite.

As an example of the analysis done to determine the phases, we describe in detail the case of Kr on a zigzag-(20,0) SWNT of radius $R = 7.8$ Å. In Fig. 1, we show the graphs of the E_{gs} and the coverage vs pressure. We first observe a rapid increase of the E_{gs} at the same pressure where the coverage steps up from $\phi = 0.01$ to 0.22. This corresponds to a transition from a vapor phase to a condensed phase (monolayer). The structure of this monolayer-film is consistent with a liquid. The film remains in a liquid phase for a wide range of pressures up to the point labeled "A" in Fig.1. At higher pressure, the E_{gs} suddenly decreases by 4.6 K due to a transition to a CS phase (points B-D). This CS phase remains stable up to $P = 2.0 \times 10^{-3}$ atm. We confirm the commensuration of the solid monolayer by calculating the 2D-RDF $g(r)$ and structure function $S(\vec{k})$, shown in Figs. 2 and 3 for isotherm points A to G. The structure seen for the isotherm point A is consistent with a liquid film. As the pressure increases the film develops a commensurate structure, consequently decreasing the energy gas–substrate. Sample configurations corresponding to isotherm points A and G are displayed in Fig. 4, where it can be appreciated the lack of structure in case A, in contrast with the order in case G. We emphasize in the figure that the 1/4-CS consists of alternated stripes of atoms in bridge and center sites. On the other hand, the 1/6 phase is an arrangement of center sites only. (see Fig. 5)

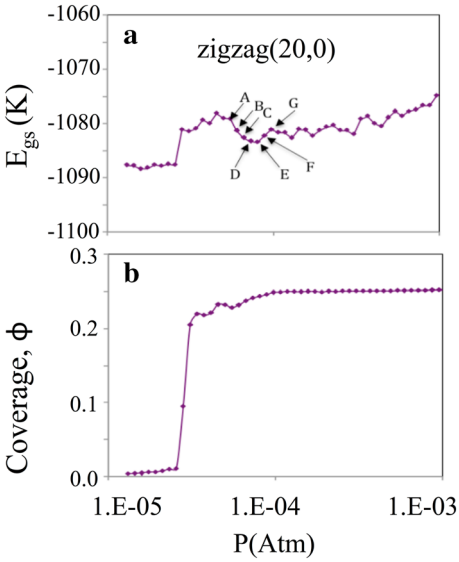

Fig. 1 Energy gas–surface (*upper panel*) and fractional coverage ϕ (*lower panel*) as a function of the pressure for Kr on a (20,0)-zigzag SWNT at 77.4 K. The labels A-G correspond to data points described in the text (Color figure online)

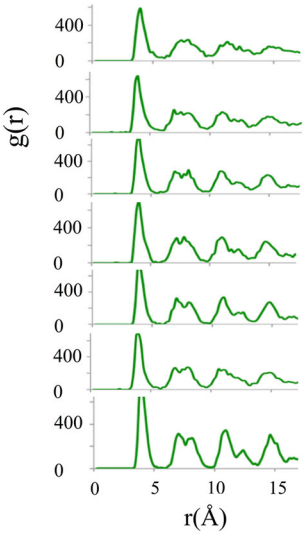

Fig. 2 2D-RDF $g(r)$ (in arbitrary units) corresponding to the isotherm points A to G (from *top* to *bottom*) as labeled in Fig. 1 (Color figure online)

The behavior of Kr on armchair SWNTs is quite different from that on zigzags. We have not found any CS phase for Kr on most armchair SWNTs considered, except for the smallest 4.74-Å-radius (7,7) tube. The transition observed in this case is from vapor to a CS of density $\phi = 0.29$. Although the coverage is slightly higher than 1/4, the lattice is similarly formed of bridge and center sites. The results for Kr on armchair SWNTs are summarized in Table 2.

Although the corrugation of the zigzag SWNTs is only slightly higher than that of the armchair ones, it is enough to trap the atoms in a CS lattice. We define the

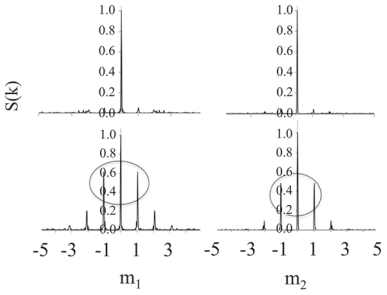

Fig. 3 Structure factor $S(k = m_1\vec{b}_1 + m_2\vec{b}_2)$ corresponding to the isotherm points A (*top*) and G (*bottom*) as labeled in Fig. 1. The *left* and *right columns* correspond to the cases $m_2 = 0$ (helical order) and $m_1 = 0$ (longitudinal order), respectively. The *ovals* emphasize the peaks at $m = \pm 1$, consistent with the CS structure. The reciprocal vectors of the 1/4-CS phase in a $(n, 0)$ zigzag nanotube are $\vec{b}_1 = (n/R_{ad}, 0)$ and $\vec{b}_2 = (n/R_{ad}, 2\pi/a)$, where, R_{ad} is the radius of the adsorbed monolayer and $a = 4.26$ Å [21]

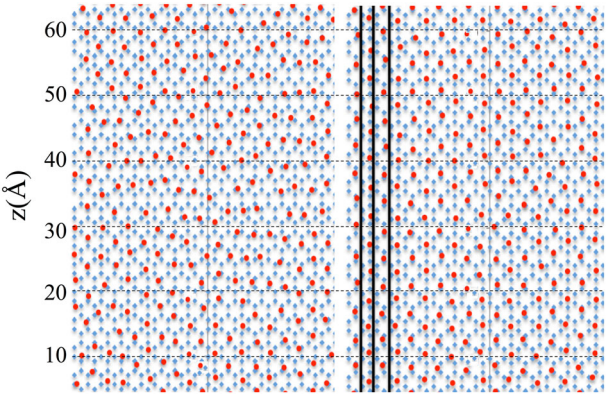

Fig. 4 Unrolled sample configurations corresponding to isotherm points A (*left*) and G (*right*). The rectangles group stripes of atoms in center and bridge sites (Color figure online)

corrugation as the difference between the potential energy of the most and least attractive sites. For example, for Kr, the corrugation of the (21,0)-zigzag and that of the (12,12)-armchair SWNTs are 119 and 16.3 K, respectively. These two SWNTs are an example of a pair of tubes with the same radius (8.2 Å) but different chirality. Due to the higher corrugation, the Kr atoms form a CS on the zigzag tube but not on the armchair one.

Given that the 1/6-CS phase is stable on graphite, we expected to find it eventually on wider tubes. However, as we see from the results displayed in Tables 1 and 2, the 1/6-CS is absent in our simulations. Only for the largest zigzag tubes we observe a monolayer with a fractional coverage starting at 1/6 (ranging from 0.16 to 0.20), which is, still, not solid. In order to explore the large radius case, we simulated Kr on a single layer of graphene, which can be considered as the infinite-radius limit of a SWNT.

The adsorption isotherms of Kr on graphene at temperatures 70, 100, and 130 K are shown in Fig. 6. At the lowest temperature, we see a stable monolayer with areal density $n = 0.065$ Å^{-2}, within 3 % of the density of the 1/6-CS phase ($n = 0.063$ Å^{-2}). We

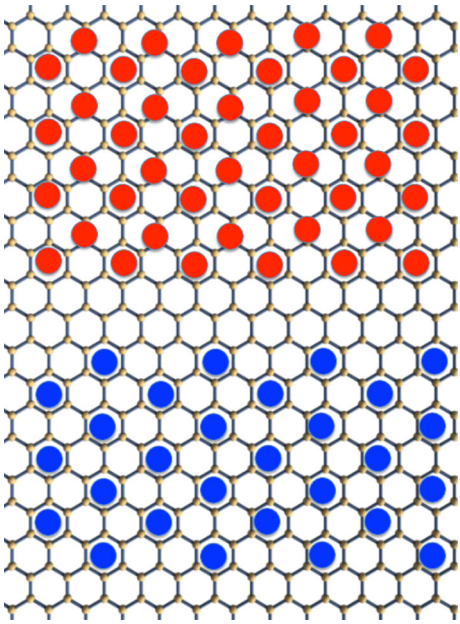

Fig. 5 Representation of the 1/4-CS (*upper red atoms*) and 1/6-CS (*lower blue atoms*) on an unrolled zigzag SWNT (Color figure online)

Table 2 Summary of the phases of Kr on armchair SWNTs at $T = 77.4$ K

Structure	Radius (Å)	Transition	Coverage (ϕ range)
Armchair (7,7)	4.74	V → CS	∼1/3(0.29)
Armchair (12,12)	8.20	V → L	∼1/4(0.21−0.26)
Armchair (13,13)	8.80	V → L	∼1/4(0.21−0.26)
Armchair (14,14)	9.50	V → L	∼1/4(0.22−0.24)
Armchair (19,19)	12.90	V → L	∼1/5(0.20−0.23)
Armchair (26,26)	17.60	V → L	∼1/5(0.18−0.21)

confirm that it is indeed a CS from the computation of the radial distribution function and the structure factors. At higher temperature, we observe an IS with a triangular lattice of density $n = 0.071$ Å^{-2}. More details of our results for Kr on graphene will be published in a forthcoming article.

4 Summary and Conclusions

To conclude, using the GCMC simulation technique we investigated the structure of Kr atoms adsorbed on suspended zigzag and armchair SWNTs with radii ranging from 4.7 to 28.83 Å. Our prediction that Kr forms a 1/4-CS phase was confirmed and extended to zigzag SWNTs of radii between 6.7 and 17.6 Å. We also observed that the 1/4-CS did not form on armchair tubes, except for the rare case of the 4.74 Å-radius (7,7) SWNT. These observations are consistent with the fact that the commensuration

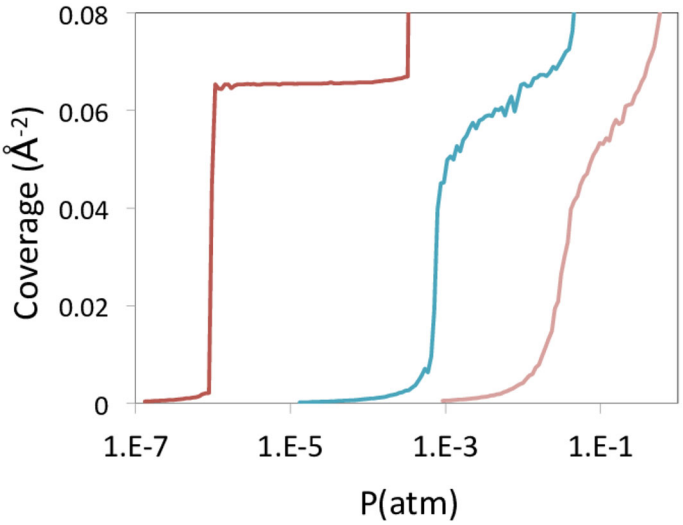

Fig. 6 Adsorption isotherms of Kr on graphene at temperatures 70, 100, and 130 K from *left* to *right* (Color figure online)

of the substrate systematically decreases with the chiral angle [22]. To complete our study, we verified that our simulations produce the expected $\sqrt{3} \times \sqrt{3}$R30° 1/6-CS phase on graphene.

These predictions are relevant to experiments where the results are interpreted based on the monolayer coverage. According to our results, a 1/4-CS should be found in experiments of Kr adsorption on SWNTs at a temperature of 77.4 K or lower.

We emphasize that the experiments reported in Ref. [17] did not actually *find* but *assume* the 1/6-CS phase. We justify this statement by quoting the authors who say "The fact that ϕ takes the value of 1/6 for the commensurate phase strongly indicates that the assumption behind Eq. 1 that $f_{\rm res} \propto \rho^{-1/2}$ is justified for this device." The assumption $f_{\rm res} \propto \rho^{-1/2}$ requires two conditions to be satisfied: (1) that the change in elastic properties is negligible compared with the fractional change in mass and (2) that the mass is distributed uniformly over the nanotube surface. Condition (1) may be achieved since the covalent CC bond is two orders of magnitude stronger than the van der Waals attraction between adsorbates. Condition (2) may be unfulfilled.

The results reported in Ref. [19] are based on the same model, $f_{\rm res} \propto \rho^{-1/2}$. We believe that the 1/4-CS is present in the results obtained in Ref. [19], where a coverage of 0.22 is reported for Ar and Kr (see Fig. S4 in [19]). Although the 1/6-CS might be stable in a wide SWNT, it is unlikely that such large SWNTs were used in the experiments reported.

Acknowledgments We are grateful for the support of the Partnership for Reduced Dimension Materials (PRDM), NSF Grant No. DMR1205608 and the Center for Integrated Quantum Materials (CIQM), NSF Grant No. DMR-1231319. We thank Milton Cole and Hye-Young Kim for fruitful comments and discussions. We thank the referees of this paper for their constructive comments.

References

1. F. Toigo, M.W. Cole, Phys. Rev. B **32**, 6989 (1985)
2. M. Boninsegni, M.W. Cole, F. Toigo, Phys. Rev. Lett. **83**, 2002 (1999)
3. F. Ancilotto, F. Toigo, Phys. Rev. B **47**, 13713 (1993)
4. M. Calbi, F. Toigo, M.W. Cole, J. Low Temp. Phys. **126**, 129 (2002)
5. A. Dillon, K. Jones, T. Bekkedahl, C. Kiang, D. Bethune, M. Heben, Nature **386**, 377 (1997)
6. A. Chambers, C. Park, R. Baker, N. Rodriguez, J. Phys. Chem. B **102**, 4253 (1998)
7. S. Inoue, N. Ichikuni, T. Suzuki, T. Uematsu, K. Kaneko, J. Phys. Chem. B **102**, 4689 (1998)
8. W. Teizer, R. Hallock, E. Dujardin, T. Ebbesen, Phys. Rev. Lett. **82**, 5305 (1999)
9. S. Weber, S. Talapatra, C. Journet, A.D. Migone, Phys. Rev. B **150**, 61 (2000)
10. M. Calbi, M. Cole, S. Gatica, M. Bojan, J.K. Johnson, in *Adsorption by Carbons*, ed. by E. Bottani, J. Tascon (Elsevier Science, Amsterdam, 2008). Chap. 9
11. A.D. Migone, in *Adsorption by Carbons*, ed. by E. Bottani, J. Tascon (Elsevier Science, Amsterdam, 2008). Chap. 16
12. S. Gatica, M. Calbi, R. Diehl, M. Cole, J. Low Temp. Phys. **152**, 89 (2008)
13. M. Calbi, M. Cole, S. Gatica, M. Bojan, G. Stan, Rev. Mod. Phys. **73**, 857 (2001)
14. S. Rols, M. Johnson, P. Zeppenfeld, M. Bienfait, O. Vilches, J. Schneble, Phys. Rev. B **71**, 155411 (2005)
15. G. Stan, M. Bojan, S. Curtarolo, S. Gatica, M. Cole, Phys. Rev. B **62**, 2173 (2000)
16. S. Gatica, M. Bojan, G. Stan, M. Cole, J. Chem. Phys. **114**, 3765 (2001)
17. Z. Wang, J. Wei, P. Morse, J. Dash, O. Vilches, D. Cobden, Science **327**, 552 (2010)
18. H.-C. Lee, O. Vilches, Z. Wang, E. Fredrickson, P. Morse, R. Roy, B. Dzyubenko, D. Cobden, J. Low Temp. Phys. **94**, 262 (2012)
19. A. Tavernarakis, J. Chaste, A. Eichler, G. Ceballos, M.C. Gordillo, J. Boronat, A. Bachtold, Phys. Rev. Lett. **112**, 196103 (2014)
20. R. Saito, G. Dresselhaus, M.S. Dresselhaus, *Physical Properties of Carbon Nanotubes* (Imperial College Press, London, 1998)
21. H. Kim, M.W. Cole, M.T. Mbaye, S.M. Gatica, J. Phys. Chem. A **115**, 7249 (2011)
22. H. Kim, E. Booth, M. Mbaye, S. Gatica, J. Low Temp. Phys. **175**, 590 (2014)
23. R. Masel, *Principles of Adsorption and Reaction on Solid Surfaces*, 1st edn. (Wiley, New York, 1996)
24. R.S. Berry, S.A. Rice, J. Ross, *Physicalchemistry* (Wiley, New York, 1980)
25. G. Stan, M.J. Bojan, S. Curtarolo, S.M. Gatica, M.W. Cole, Phys. Rev. B **62**, 2173 (2000)
26. W. Carlos, M. Cole, Surface Sci. **91**, 339 (1980)
27. L. Bruch, M. Cole, E. Zaremba, *Physical Adsorption: Forces and Phenomena* (Dover Publications, Mineola, 2007)